Proc. Natl. Acad. Sci. USA
Vol. 78, No. 11, pp. 7200–7204, November 1981
Neurobiology

Kinetic parameters for acetylcholine interaction in intact neuromuscular junction

(α-bungarotoxin/voltage clamp/binding kinetics/acetylcholine receptor)

BRUCE R. LAND†, EDWIN E. SALPETER‡, AND MIRIAM M. SALPETER†§

†Section of Neurobiology and Behavior, Division of Biology, and Departments of ‡Physics and §Applied Physics, Cornell University, Ithaca, New York 14853

Contributed by E. E. Salpeter, August 3, 1981

ABSTRACT **The dependency of miniature endplate current (mepc) rise time upon mepc amplitude and acetylcholine receptor site density was measured in lizard intercostal muscles and used to fit the rate constants in a simple kinetic scheme. The kinetic scheme included diffusion, two-step sequential binding of acetylcholine to receptor, and opening of the ion channel. Numerical simulation of the observed mepc behavior yielded the following kinetic constants: (*i*) diffusion constant, 4×10^{-6} cm^2 sec^{-1}; (*ii*) forward binding rates, 4.7×10^7 M^{-1} sec^{-1}; (*iii*) channel relaxation rate, 25 msec^{-1}. The value above for the forward binding rates assumed both rates to be equal. If they are different, the slower of the two is in the range of 2–5 $\times 10^7$ M^{-1} sec^{-1}. A radial profile of bound receptor indicated that activation of the receptor was very local, occurring essentially within a radius of about 0.3 μm from the point of acetylcholine release.**

The vertebrate neuromuscular junction is one of the fastest known synapses. In lizard muscles, the 20–80% rise time (t_r) for the miniature endplate current (mepc) in response to a quantum of acetylcholine (AcCho) is less than 100 μsec (1). It is of interest to determine what molecular specializations are responsible for this rapid transmitter action. Three processes have been considered as potential rate-limiting factors: diffusion of AcCho from its point of release to its postsynaptic receptors, binding of AcCho to receptors, and opening of ion channels in the muscle membrane subsequent to AcCho binding. Treated as a chemical kinetic problem, variation of the concentrations of the reactants in the system during the reaction time course should provide information about the rate-limiting steps. Decreasing the receptor density (σ) by partial inactivation with α-bungarotoxin (BTX) allowed us to account quantitatively for the σ-dependent processes (binding, diffusion, or both) and the σ-independent processes (e.g., channel opening) that contribute significantly to t_r (1). In this paper, we use the naturally occurring variation in the amount of AcCho in a "quantum," as reflected in the variation in the mepc amplitude to determine the separate contributions of binding and diffusion to t_r. We show that, from the slope of mepc amplitude versus t_r, one can separate the contributions of binding and diffusion and thus obtain values for the association rate of AcCho for its receptor and for the diffusion constant of AcCho in the synapse. Furthermore, we can evaluate the extent to which the AcCho of one quantum locally saturates the receptors in a small area opposite the point of release (2–6).

METHODS

In an earlier study (1), to be referred to as paper I, we used three groups of lizard (*Anolis carolinensis*) intercostal muscle, each with a different concentration of AcCho receptor (AcChoR) sites: the AcChoRs were either left intact or partially inactivated with nonradioactive BTX (40 nM) for 20 or 40 min. To simplify the system, the esterases were inactivated with diisopropyl fluorophosphate (1 mM for 30 min). After thorough washing, mepcs were recorded by voltage clamp set at 100 mV. When the physiological measurements were completed, the muscles were saturated with ^{125}I-labeled BTX (500 nM) for 2 hr (3) and AcChoR site density (σ) was determined by electron microscopic autoradiography as described (1).

In the present paper, the experimental conditions were identical to those in paper I except that we modified the voltage clamp filtering conditions slightly. In the control neuromuscular junction (unpoisoned by BTX), we still used a 4-kHz filter cutoff to produce minimum distortion of mepc rise time. However, for the smaller but slower mepcs from lower σ preparations, we could improve the signal-to-noise ratio without a major distortion of the rise time by using a 3-kHz cutoff.

KINETIC SCHEME, DEFINITIONS, AND ASSUMPTIONS

We consider the following kinetic scheme (7):

$$\text{(AcCho release} \xrightarrow{D} \text{AcCho diffusion)}$$

$$2\,\text{AcCho} + \text{R}_\text{c} \underset{k_{-1}}{\overset{2k_{+1}}{\rightleftharpoons}} \text{AcCho} + \text{AcCho-R}_\text{c} \underset{2k_{-2}}{\overset{k_{+2}}{\rightleftharpoons}} (\text{AcCho})_2\text{-R}_\text{c} \underset{l_-}{\overset{l_+}{\rightleftharpoons}} (\text{AcCho})_2\text{-R}_\text{c}^*, \qquad [1]$$

in which D is the diffusion constant; R_c and R_c^* are the AcChoR channel complex, with the channel in the closed and open conformation, respectively; k_{+1} and k_{+2} are the two forward binding rate constants; k_{-1} and k_{-2} are the two unbinding rate constants; and l_+ and l_- are the channel conformation change rate constants.

The following assumptions and definitions will be made (except when otherwise indicated):

(*i*) We will equate one BTX binding site with one AcCho binding site (AcChoR) (8) and will assume that there are two AcChoRs per AcChoR channel complex (R_c) and that each R_c has to be occupied by AcCho to open the channel (1, 4, 9–12).

(*ii*) We assume no cooperativity in forward binding—i.e., $k_{+1} = k_{+2}$ and both forward rate constants will be referred to as k_+.

(*iii*) Due to a very high initial AcCho concentration in the cleft, the back reactions are assumed to be slow relative to the

The publication costs of this article were defrayed in part by page charge payment. This article must therefore be hereby marked "*advertisement*" in accordance with 18 U. S. C. §1734 solely to indicate this fact.

Abbreviations: mepc, miniature endplate current; AcCho, acetylcholine; AcChoR, AcCho receptor; BTX, α-bungarotoxin; σ, AcChoR site density (sites per μm^2 of membrane surface area).

forward rates of AcCho binding and gate opening. The rising phase of a mepc will thus be controlled primarily by D, k_+, and the relaxation rate for gate opening ($l_+ + l_-$).

(*iv*) The mepc amplitude A_c is given by:

$$A_c = (0.5N)gF\gamma V, \quad [2]$$

in which V (= 100 mV) is the clamped membrane potential; γ is the conductance per single channel [taken to be 25 pS (13)] F is an "efficiency factor" for double binding, defined as the fraction of AcCho molecules that are on doubly bound R_cs at peak amplitude; g is the fraction of doubly bound R_cs that have an open channel [$g = l_+/(l_+ + l_-)$]; and N, which is the number of AcCho molecules per quantal packet, is multiplied by 0.5 because of assumption *i*.

(*v*) The quantal area a_q is defined as the postsynaptic area that contains the number of AcCho binding sites equal to N; thus, $a_q = N/\sigma$.

(*vi*) We assume that after a point release of a quantal packet of AcChoR, half of the quantal packet diffuses in the primary cleft in both directions along the adaxonal surface of the postjunctional membrane (receptor concentration = σ) while the second half diffuses into the secondary cleft, where two facing sheets of receptor-rich membrane extend ≈2500 Å from the top (2).

(*vii*) Two limiting times were defined in our previous paper (1): First is a diffusion time t_d, for diffusion over area a_q. (Due to assumption *vi*, t_d will be considered as the time to diffuse simultaneously over two disks each of area 0.5 a_q.) Second is a "nominal" binding time t_b for the binding of a single AcCho molecule to AcChoR (no competition for binding). These definitions (with a numerical modification discussed below) were:

$$t_d = \frac{0.8}{4\pi} \times \frac{0.5N}{\sigma D} \quad [3]$$

and

$$t_b = \frac{1.39h}{1.5\sigma k_+}, \quad [4]$$

in which k_+ is the forward binding rate constant and h is the width of the cleft (σ/h is the effective concentration of AcChoR in the primary cleft). The factor 1.39 is the conversion factor for t_b from *e*-folding time to 20–80% rise time. The factors 1.5 and 0.5 take into consideration the junctional fold geometry (assumption *vi*): 0.5 for the two half disks and 1.5 for the double layer of receptor down the folds.

The factor of 4π comes from the conventional definition for diffusion time being $r^2/4D$ = area/$4\pi D$ (r being a radius), and 0.8 is the conversion factor to 20–80% rise time calculated for conditions when diffusion is rate limiting.

(*viii*) The 20–80% rise time is approximated by:

$$t_r = [t_c^2 + (t_{b+d})^2]^{1/2}, \quad [5]$$

in which t_{b+d}, to be called the "reduced rise time," is the combined contribution from diffusion plus binding, and t_c, the σ-independent time delay, which is assumed to be primarily the "gate opening time." The summing of t_c and t_{b+d} as the square root of the sum of their squares was obtained empirically (1) to give a simple relationship that best fit the calculated convolution of two independent time courses: one an isomerization relaxation and the other the solution to the diffusion and binding equations for 20–80% reduced rise time.

RESULTS

Fig. 1 shows the distribution of mepc amplitude under the AcChoR site density conditions used. It indicates that we did not lose many low amplitude mepcs due to a low signal-to-noise ratio even in the muscles most extensively treated with BTX (40 min).

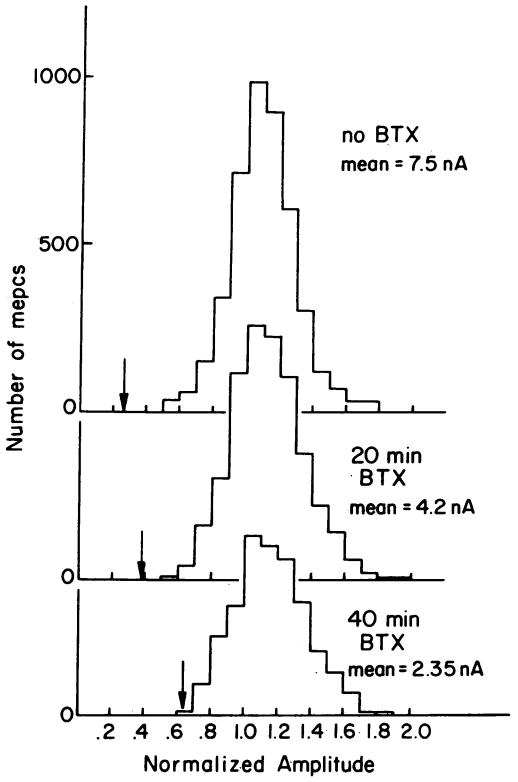

FIG. 1. Amplitude histograms for each of the three σ conditions. A total of 3000–4000 mepcs is included for each experimental σ. For comparison, the three distributions were scaled to their own mean. The similarity in shape of all three distributions shows that, although our low-amplitude data (40 min BTX) were close to the recording noise level (indicated by arrows), we did not bias our sample by losing any significant number of the smallest amplitude mepcs.

Table 1 gives average values for t_r, A_c, and σ similar to those in paper I but based on about 30% more animals. Fig. 2 shows the experimental results of the dependence of t_r on A_c for each of the three AcChoR site densities. An overall measure of the rise time amplitude dependence is the mean linear slope (dt_r/dA_c) for each of the three conditions in Fig. 2. The linear slope values are given in Table 1, showing a strong increase with decreasing σ (slightly stronger than $1/\sigma^2$). This strong dependence is expected from the results in paper I, which showed that t_r is almost proportional to $1/\sigma$ and A_c to σ. The fact that dt_r/dA_c depends on σ more strongly than $t_r/A_c \propto 1/\sigma^2$ is again expected if the gate opening time t_c is independent of σ (1) and thus contributes a larger proportional effect for the shorter rise time in endplates with higher σ.

Previously (1), we found t_c to be 58 μsec. When we factor out the contributions of t_c to t_r (using Eq. 5) and plot the resultant reduced rise time, t_{b+d}, against amplitude on logarithmic scales (Fig. 3), we obtain a mean slope:

$$\beta = \frac{d\ln(t_{b+d})}{d\ln(A_c)} = \frac{dt_{b+d}}{dA_c} \Big/ \frac{t_{b+d}}{A_c}, \quad [6]$$

which is dimensionless. Thus, in the relationship $t_{b+d} = k\sigma^\alpha A_c^\beta$, the logarithmic slope, β, eliminates the effect introduced by σ on the linear slope. Table 1 gives the β values obtained for our three experimental conditions.

The most important experimental result of the present paper is that β is greater than 0 and less than 1. This means that both

Table 1. Average AcChoR densities, amplitudes, and rise times (20–80%) of mepc at three different BTX treatment levels

BTX treatment, min	σ,* sites/μm^2	Mean amplitude,† nA	Mean rise time, μsec	Slope of time vs. amplitude, μsec/nA	β
0	15,300 ± 3000	7.5 ± 1.3	95 ± 15	0.92	0.6
20	7,700 ± 1500	4.2 ± 0.7	147 ± 25	8.4	0.3
40	5,450 ± 1000	2.35 ± 0.5	193 ± 25	44.0	0.6

See Figs. 2 and 3 for plotted data. Data are presented ±SEM.

* AcChoR site densities are systematically 10% lower than given in paper I because they were corrected for receptors at the bottom of the folds. Data were based on 18 animals, 72 fibers, and 2800 developed grains. All animals used for autoradiography had been first used for physiological measurements. However, autoradiography and physiological measurements were not performed on the same fibers.

† Physiological measurements were based on 36 animals.

diffusion and binding are important in determining the rise time. If diffusion were rate limiting, t_d (from Eq. 3) would dominate t_{b+d} and β would be 1; and if binding were rate limiting, t_b (of Eq. 4) would be t_{b+d} and β would be 0. Qualitatively, this can be seen from the argument that if diffusion is much slower than binding, then binding can occur over the area a_q. F then approaches unity and the rise time is proportional to N and thus the amplitude. If binding is slow, then t_b dominates the rise time, and because t_b (Eq. 4) is independent of N, the rise time would then be independent of amplitude.

Derivation of Kinetic Constants. We used a computer program similar to that of Wathey *et al.* (4) (to be described in detail elsewhere) to solve the coupled differential equations for diffusion and binding with the isomerization step accounted for as in Eq. 5.

In general, for any assumed value of k_+ and D and the experimental values of σ, N is varied to get a t_r versus A_c relationship. We then compared these to our experimental values by a maximum likelihood procedure (Fig. 4). We initially used the t_c value of 58 μsec obtained in paper I. t_c was then allowed to vary to maximize the fit between the observed and derived rise times. The best-fit t_c was found to be 55 μsec [and thus within experimental error of that obtained previously (1)].

Best-fit values are given in Table 2, and the predicted t_{b+d} versus A_c are plotted for each condition of σ as the smooth curves in Fig. 3.

Table 3 shows the effect on the derived best-fit parameters values (without error ranges) for varying some of our initial assumptions. In part A, positive or negative cooperativity in binding (k_{+2}/k_{+1} = 10 and 0.1) is assumed; in part B a reasonable set of back reactions (15) is assumed. The maximum likelihood procedure did not yield sufficiently poorer fits for any of the ratios of k_{+1}/k_{+2} to give any reliable information on whether there is any cooperativity in binding. However, the slower of k_{+1} or k_{+2} was within about a factor of 2 of the value given as k_+ in Table 2. Table 3*B* shows that the resultant best fit values of N, k_+, and D with back reactions are within the error range of values given in Table 2.

DISCUSSION

We obtained values for the rate constants of AcCho diffusion (D) and binding (k_+) to AcChoR in the cleft of the lizard neuromuscular junction under conditions of AcCho release and delivery prevailing during normal mepcs. By experimentally determining the correlation between rise time and amplitude of mepcs, for various conditions of AcChoR site density in esterase inactivated endplates, we could compare these experimental results with those predicted from numerical solutions modeling diffusion and binding. We find that the three processes, AcCho diffusion, AcCho binding, and AcChoR gate opening, all contribute to the mepc rise time; that is, there is no single rate-limiting step.

Comparison of Kinetic Parameters with Values Reported in the Literature. (*i*) Our value for the diffusion constant of AcCho in the synaptic cleft, 4 (+3, −2) × 10^{-6} cm^2 sec^{-1}, is close to that of free diffusion (≈8 × 10^{-6} cm^2 sec^{-1}) (14). It is in line with the value used by Wathey *et al.* (4) to fit mepc time

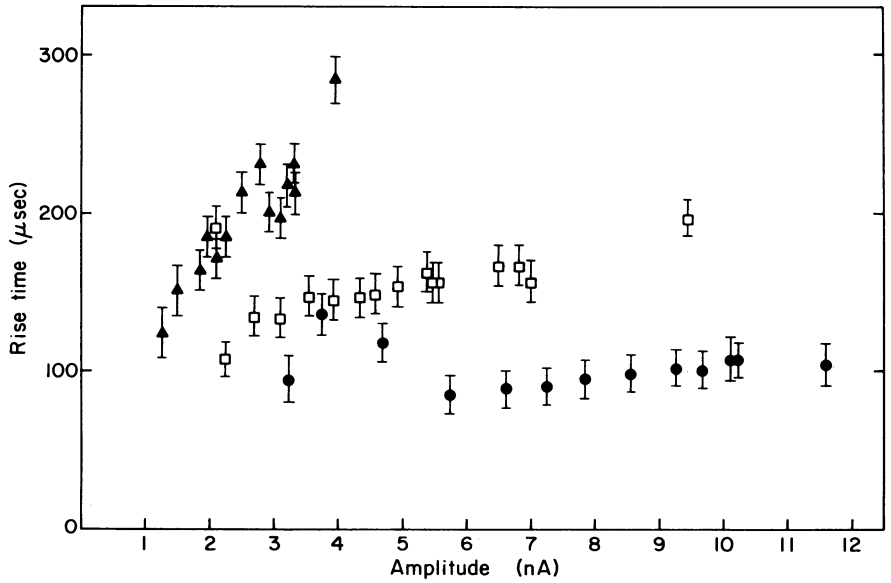

FIG. 2. mepc 20–80% rise time vs. amplitude at three different AcChoR site densities. The extreme right and left amplitude bins for each density represent relatively few mepcs (see Fig. 1). Data for each density show a positive correlation of rise time with amplitude. Error ranges represent the summing of three independent errors, due to (*i*) noise remaining on averaged traces, (*ii*) possible misalignment of traces during averaging, and (*iii*) time quantization error. Three experimental conditions: ●, No BTX; □, 20 min in BTX; ▲, 40 min in BTX.

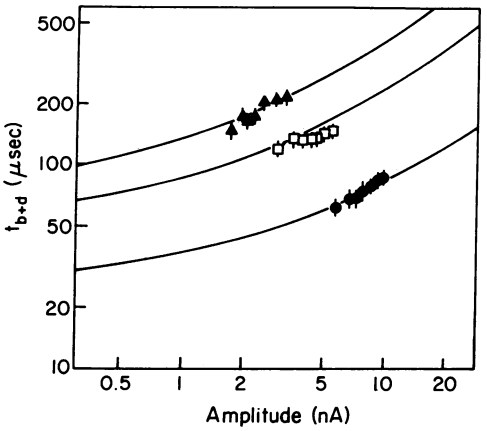

FIG. 3. After averaging the lowest bins represented in Fig. 2, data were converted to reduced rise time t_{b+d}, derived from Eq. 5 with t_c = 58 μsec (from paper I), plotted logarithmically against mepc amplitude. The three sets of points are labeled as in Fig. 2. The three solid lines are the expected amplitude versus t_{b+d} curve for $k_+ = 4.7 \times 10^7$ M^{-1} sec^{-1} and $D = 4 \times 10^{-6}$ cm^2 sec^{-1}. Note that the slopes of the theoretical curves are small ($\beta \ll 1$) for low mepc amplitude and approach a constant ($\beta = 1$) for high mepc amplitudes. The experimental points cluster on the theoretical curve at intermediate values of β.

course and that estimated by Krouse (16) to account for voltage-jump results.

(*ii*) Our value for $t_c = 1.39/(l_+ + l_-)$ of ≈55 μsec is appreciably shorter than that given by the relaxation rates estimated by others (6, 17, 18), with the exception of that in the squid stellate ganglion given by Llinás *et al.* (19). It is not clear whether the differences are due to species, to the techniques used, or to the assumption about kinetic models.

(*iii*) Our measured value for $k_{+1} = k_{+2}$ of $4.7\ (+5, -3) \times 10^7$ M^{-1} sec^{-1} is within the range of 10^7–10^8 given by others for the binding step (4, 20).

(*iv*) The results in Table 2 give us a value for $N \times g$, but we have no direct manner of obtaining either value alone. It is therefore of interest to speculate on the most likely value of N and g. As can be seen from Table 2, g affects the values of both N and D. Several arguments can be made for believing that g (the efficiency of opening the ion channel in doubly bound R_c) is close to unity. First, if we assume $g = 1$, then our value for N is 10,000 ± 3600 molecules per quantum (Table 2), the value given by Kuffler and Yoshikami (21) as a probable upper limit. Any decrease in g would require a larger N. More compelling, however, is the fact that D is near free diffusion. A value of g much less than 0.3 would increase D to well above free diffusion. Values for g ranging between 0.4 and 0.9 are given in the literature (15, 22).

Table 2. Best-fit values*

$k_1 = k_2 = 4.7\ (+5, -3) \times 10^7$ M^{-1} sec^{-1}
$D^\dagger = 4\ (+3, -2) \times 10^{-6}$ cm^2 sec^{-1}/g
$1/(l_+ + l_-) = 40\ (\pm 15)$ μsec
$N^\dagger$ = 10,000 (±3600) molecules/g
$F = 0.6\ (\pm 0.2)$
$t_d \approx 50\ (+25, -15)$ μsec
$t_b \approx 40\ (+40, -20)$ μsec
$t_c \approx 55\ (\pm 25)$ μsec

Best-fit values were obtained as described in Fig. 4. Error ranges are greatly reduced if either k_+ or D is assumed and the other is calculated from the equation of the crest line given in the legend of Fig. 4. For instance, if D were precisely 8×10^{-6} (a possible value for free diffusion) (14), then $k_+ = (2.9 \pm 0.4) \times 10^7$ M^{-1} sec^{-1}.

* We also obtained separate best-fit values for each of the three experimental conditions of σ separately and found them to be within the error range of these values.

† Note that we get explicitly only $N \times g$ and $D \times g$.

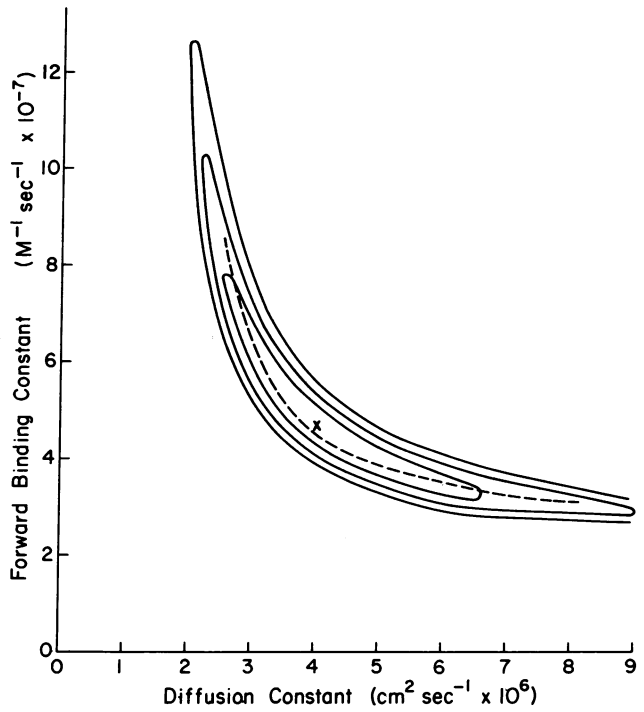

FIG. 4. Contours representing the total probability for obtaining the observed or greater difference between the experimental and predicted rise times as a function of different values for k_+ (ordinate) and D (abscissa). Results were obtained from approximately 1000 combinations of k_+ and D for each of 21 experimental values of A_c (seven values for each of three conditions of σ). The best-fit value of t_c = 55 μsec was used. The center cross marks the best fit (i.e., the k_+/D combination that gives the largest probability). Each contour represents an equal probability deviation from the best fit. The three contours represent a decrease in probability to $1/e^2$, $1/e^4$, and $1/e^6$, respectively. The center "crest line" is the best value of D for various values of k_+ fit by following equation:

$$\frac{(0.52)\ (4.7 \times 10^7)}{k_+} + \frac{(0.46)\ (4 \times 10^{-6})}{D} = 1 \pm 0.15.$$

This leads to an appreciably smaller uncertainty in deriving either k_+ or D if the other parameter is known (or assumed), using the relationship of the crest line in which k_+ is in units of M^{-1} sec^{-1} and D is in units of cm^2 sec^{-1}.

"Saturated Disk Model." When the nerve is stimulated at a neuromuscular junction, it releases ≈200–300 quantal packets of AcCho (5). On various grounds, several investigators have suggested that (under normal conditions), the postsynaptic

Table 3. Kinetic constants under various assumptions

Assumption	k_1, M^{-1} sec^{-1} × 10^{-6}	k_2, M^{-1} sec^{-1} × 10^{-6}	$g \times D$, cm^2 sec^{-1} × 10^6	$g \times N$	F
		A. Varying cooperativity			
$k_1 = k_2$	47	47	4.0	10,000	0.62
$k_2 = 10k_1$	20	200	2.2	7,800	0.77
$k_2 = 0.1k_1$	170	17	3.6	13,600	0.44
		B. With back reactions			
$k_d = 40$ μM					
$g = 0.7$*	40	40	3.6	10,700	0.61

* Ref. 15.

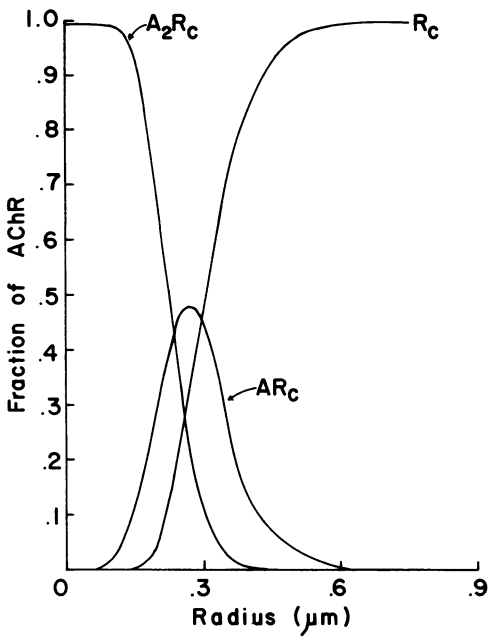

FIG. 5. Radial density profiles away from AcCho release site for AcCho receptor (AChR)–channel complexes at 90% mepc peak: with no AcCho (R_c), one AcCho (AR_c), and two AcCho (A_2R_c) molecules per complex. Ordinate is relative to total receptor–channel density. The curves are based on the kinetic model and the best-fit parameters from Table 2. The density of doubly bound complexes (A_2R_c) drops to 10% by 0.3 μm (which is the radius of the unit disk $\frac{1}{2}a_q$). Integrating this curve shows that 95% of A_2R_c are within that radius, 0.3 μm, or that 57% of all receptor–channel complexes within a_q are doubly bound.

membrane areas acted on by different quantal packets do not overlap with each other, and each is acted on at saturating AcCho concentrations (2–6). In previous publications (2, 3) we argued that the AcCho concentration acting over the postsynaptic area a_q is given by the AcChoR site density. This gives a concentration >500 μM and thus ≈15 times higher than a typical value for the equilibrium dissociation constant of ≈30 μM (15). However, even though the AcCho concentration is saturating, the extent to which the AcChoRs within the postsynaptic area (a_q) are saturated with AcCho depends primarily on the ratio of binding time to diffusion time. In paper I, we argued that complete saturation would pertain if $t_d/t_b \gg 1$. Then all the AcCho can in principle be bound within a minimum area (a_q). All the receptors will be doubly bound (F will approach 1), and the systems will be most efficient. Conversely, if $t_d/t_b \ll 1$, then even if AcCho is at saturating concentrations, it will spread over an area considerably larger than a_q. A considerable number of receptors will be unbound or singly bound by AcCho (F will be small), and the systems will be more wasteful of AcCho if (as given in assumption *i*) it takes two AcCho molecules per A_c to open the channel (1, 4, 11, 12).

Fig. 5 shows that less than 5% of the doubly bound receptors are seen beyond 0.3 μm and virtually none beyond 0.5 μm from the point of release of AcChoR. It is of interest to note that AcChoR is at high density ≈0.2–0.3 μm down the folds.

Because we are assuming that only doubly bound AcChoRs open the ion channel, 0.3 μm defines the effective radius around the release site within which the AcCho quantum opens ion channels. This result demonstrates that binding is fast enough to keep pace with diffusion, such that the AcCho can indeed be bound within a small postsynaptic area.

We thank Drs. Paul Adams, Charles Stevens, Jonathan Cohen, and Stephen Jones for helpful suggestions, Maria Szabo and Mary Johnson for technical assistance, and Polly Marion for typing the manuscript. This work was supported by National Institutes of Health Grant NS09315 (to M.M.S.) and a Muscular Dystrophy Postdoctoral Fellowship (to B.R.L.).

1. Land, B. R., Salpeter, E. E. & Salpeter, M. M. (1980) *Proc. Natl. Acad. Sci. USA* **77**, 3736–3740.
2. Fertuck, H. C. & Salpeter, M. M. (1976) *J. Cell Biol.* **69**, 144–158.
3. Matthews-Bellinger, J. & Salpeter, M. M. (1978) *J. Physiol.* **279**, 197–213.
4. Wathey, J. C., Nass, M. M. & Lester, H. A. (1979) *Biophys. J.* **27**, 145–164.
5. Hartzell, H. C., Kuffler, S. W. & Yoshikami, D. (1975) *J. Physiol.* **251**, 427–463.
6. Adams, P. R. (1980) in *Information Processing in the Nervous System*, eds. Perisker, H. M. & Willis, W. D., Jr. (Raven, New York).
7. Adams, P. R. (1977) *J. Physiol. (London)* **268**, 271–289.
8. Neubig, R. R. & Cohen, J. B. (1979) *Biochemistry* **24**, 5464–5475.
9. Neubig, R. R. & Cohen, J. B. (1980) *Biochemistry* **19**, 2770–2779.
10. Sine, S. M. & Taylor, P. (1980) *J. Biochem.* **255**, 10144–10156.
11. Dionne, V. E., Steinbach, J. H. & Stevens, C. F. (1978) *J. Physiol.* **281**, 421–444.
12. Sheridan, R. E. & Lester, H. A. (1977) *J. Gen. Physiol.* **70**, 187–219.
13. Colquhoun, D., Dionne, V. E., Steinbach, J. H. & Stevens, C. F. (1975) *Nature (London)* **253**, 204.
14. Dionne, V. E. (1976) *Biophys. J.* **16**, 705–717.
15. Adams, P. R. (1981) *J. Membr. Biol.* **58**, 161–174.
16. Krouse, M. E. & Lester, H. A. (1981) *Biophys. J.* **33**, 15a (abstr.).
17. Adler, M., Albuquerque, E. X. & Lebeda, F. J. (1978) *Mol. Pharmacol.* **14**, 514–529.
18. Grundhagen, H.-H., Iwatsubo, M. & Changeux, J.-P. (1977) *Eur. J. Biochem.* **80**, 225–242.
19. Llinás, R., Steinberg, I. Z. & Walton, K. (1981) *Biophys. J.* **33**, 323–352.
20. Neumann, E. & Chang, H. W. (1976) *Proc. Natl. Acad. Sci. USA* **73**, 3994–3998.
21. Kuffler, S. W. & Yoshikami, D. (1975) *J. Physiol.* **251**, 465–482.
22. Cash, D. J., Aoshima, H. & Hess, G. P. (1981) *Proc. Natl. Acad. Sci. USA* **78**, 3318–3322.